

Imaging single membrane fusion events mediated by SNARE proteins

Marina Fix*, Thomas J. Melia†, Jyoti K. Jaiswal*, Joshua Z. Rappoport*, Daoqi You†, Thomas H. Söllner†, James E. Rothman†, and Sanford M. Simon**

*Laboratory of Cellular Biophysics, The Rockefeller University, 1230 York Avenue, Box 304, New York, NY 10021; and †Cellular Biochemistry and Biophysics Program, Memorial Sloan-Kettering Cancer Center, 1275 York Avenue, Box 251, New York, NY 10021

Contributed by James E. Rothman, March 12, 2004

Using total internal reflection fluorescence microscopy, we have developed an assay to monitor individual fusion events between proteoliposomes containing vesicle soluble *N*-ethylmaleimide-sensitive factor attachment protein receptors (SNAREs) and a supported planar bilayer containing cognate target SNAREs. Approach, docking, and fusion of individual vesicles to the target membrane were quantified by delivery and subsequent lateral spread of fluorescent phospholipids from the vesicle membrane into the target bilayer. Fusion probability was increased by raising divalent cations (Ca^{2+} and Mg^{2+}). Fusion of individual vesicles initiated in <100 ms after the rise of Ca^{2+} and membrane mixing was complete in 300 ms. Removal of the N-terminal H_{abc} domain of syntaxin 1A increased fusion probability >30-fold compared to the full-length protein, but even in the absence of the H_{abc} domain, vesicle fusion was still enhanced in response to Ca^{2+} increase. Our observations establish that the SNARE core complex is sufficient to fuse two opposing membrane bilayers at a speed commensurate with most membrane fusion processes in cells. This real-time analysis of single vesicle fusion opens the door to mechanistic studies of how SNARE and accessory proteins regulate fusion processes *in vivo*.

Most intracellular fusion is believed to be mediated by soluble *N*-ethylmaleimide-sensitive factor attachment protein receptor (SNARE) proteins assembled into SNAREpins (trans SNARE complexes). SNARE motifs of vesicle (v-) and target (t-) SNARE proteins align in parallel orientation and form a coiled-coil structure that bridges opposing membranes and brings them in close proximity, allowing for their fusion. Inhibition of fusion by SNARE-specific toxins and inhibitory peptides (1, 2) and fusion of cells expressing cognate SNAREs in flipped topology (3) provide evidence in favor for the fusogenic role of SNAREs. Biochemically, SNARE function has been assayed by using the fluorescence dequenching assay (4), where purified neuronal v- and t-SNARE proteins are reconstituted into distinct populations of liposomes. Dequenching of phospholipid dyes present in only one liposome population is used as readout of membrane bilayer mixing, thus fusion (4). Because macroscopic dequenching may fail to report subtle changes that can occur at the level of single v-SNARE proteoliposomes (v-liposomes), the ability to monitor individual vesicles during fusion would provide better insight into the various steps and their regulation during SNARE-mediated membrane fusion.

Total internal reflection fluorescence microscopy (TIR-FM) has been used to study fusion of single vesicles *in vivo* (5–10) and viral-mediated fusion *in vitro* (11). These experiments have demonstrated the benefits of a spatially restricted excitation in the evanescent field to visualize fusion of single exocytic vesicles at high spatial and temporal resolution.

By using TIR-FM, we have developed an assay to investigate SNARE-mediated fusion of single v-liposomes to target bilayers and used it to evaluate the probability and rate of vesicle fusion under various conditions, including the effects of divalent cations and the N-terminal H_{abc} domain of syntaxin 1A.

Materials and Methods

Proteoliposome Preparation. Full-length SNARE protein expression and purification were performed as described (4, 12). Syntaxin without the N-terminal H_{abc} domain was generated by PCR from pTW34 (4) with the primers tm65 (ATACCGAGATCTTCATCCAAAGATGCCCGATGG) and tm66 (ACATGACCATGGAGAGGCAGCTGGAGATCAC). The resulting product was cut with *Nco*I and *Bam*HI and ligated into pET 28a to form pTM10. The expressed protein consists of syntaxin with its first 150 amino acids deleted and replaced by Met and Glu. It is missing the entire H_{abc} domain but retains the linker region and SNARE and transmembrane domains. This protein was coexpressed with synaptosomal-associated protein (SNAP)-25 and the complex purified via the his-tag on SNAP-25.

Purified v-SNARE vesicle-associated membrane protein 2 (VAMP-2) was reconstituted in 82 mol% 1-palmitoyl-2-oleoyl-*sn*-glycero-3-phosphatidylcholine (POPC), 15 mol% 1,2-dioleoyl-*sn*-glycero-3-phosphatidylserine (DOPS), and lissamine rhodamine B- (Rh-) and 7-nitrobenz-2-oxa-1,3-diazole (NBD)-tagged 1,2-dipalmitoyl-*sn*-glycero-3-phosphatidylethanolamine (DPPE), 1.5 mol% each, as described (4). All phospholipids and lipid dyes were purchased from Avanti Polar Lipids. v-liposomes were stored at -80°C and diluted at least 1:40 before use with a 25 mM Hepes/100 mM KCl, pH 7.4/KOH buffer.

Purified t-SNAREs (SNAP-25 and syntaxin with a thrombin cleavage site at amino acid 181) were reconstituted into POPC proteoliposomes without Nycodenz ultracentrifugation, as described (13).

Supported Bilayer Preparation. t-SNARE proteoliposomes were diluted with buffer to a final lipid concentration of 100 μM , added to cleaned glass coverslips (diameter 25 mm, Fisher Scientific) in Sykes-Moore chambers (Bellco Glass), and incubated at room temperature (RT) for ≈ 2 h while being protected from the light. Proteoliposomes composed of SNAP-25 and syntaxin without H_{abc} domain were incubated on glass coverslips for ≈ 1 h at RT. Longer incubation times resulted in reduced activity of target bilayers.

The target bilayers were rinsed 10 times by repeatedly adding and removing 1 ml of buffer. The final volume in the chamber was ≈ 1 ml. The bilayers were used immediately after preparation.

Supported planar bilayers without t-SNAREs were prepared as described above with the following change: pure POPC small

Abbreviations: SNARE, soluble *N*-ethylmaleimide-sensitive factor attachment protein receptor; v-SNARE, vesicle SNARE; t-SNARE, target SNARE; v-liposome, v-SNARE proteoliposome; NBD, 7-nitrobenz-2-oxa-1,3-diazole; POPC, 1-palmitoyl-2-oleoyl-*sn*-glycero-3-phosphatidylcholine; Rh, lissamine rhodamine B; DPPE, 1,2-dipalmitoyl-*sn*-glycero-3-phosphatidylethanolamine; RT, room temperature; SUVs, small unilamellar vesicles; TIR-FM, total internal reflection fluorescence microscopy; SNAP-25, synaptosomal-associated protein of 25 kDa; VAMP, vesicle-associated membrane protein.

†To whom correspondence should be addressed. E-mail: simon@rockefeller.edu.

© 2004 by The National Academy of Sciences of the USA

unilamellar vesicles (SUVs) were used instead of t-SNARE proteoliposomes. SUVs were prepared by depositing POPC in chloroform into a round-bottom glass tube and removing chloroform under a stream of argon gas. The phospholipid film was kept under vacuum for at least 2 h, then hydrated with buffer (25 mM Hepes/100 mM KCl, pH 7.4/KOH, final phospholipid concentration 1 mg/ml), equilibrated for 5 min at RT, and vortexed three times for 10 s to form multilamellar vesicles. SUVs were prepared from multilamellar vesicles by bath sonication (Laboratory Supplies, Hicksville, NY) at RT for 15–20 min. The SUV suspension was diluted with buffer to 100 μ M, added onto cleaned glass coverslips in Sykes–Moore chambers, and incubated at RT. The phospholipid bilayer was rinsed 10 times with buffer as described above and used immediately.

Formation of supported bilayers was checked initially by fluorescence recovery after photobleaching of NBD-DPPE incorporated into the supported bilayer in TIR mode by using a 442-nm laser (Omnichrome HeCd laser series 56 with power supply LC-500, Melles Griot, Irvine, CA; 442/515dc dichroic mirror, emission 525/50 band-pass filter, both from Chroma Technology, Brattleboro, VT). A small area of the bilayer was bleached for 5 s and recovery monitored in time-lapse mode (METAMORPH, Universal Imaging, Downingtown, PA) every 30 s for \approx 5 min. The diffusion coefficient for NBD-DPPE in supported t-SNARE bilayers was in good agreement with the value for a pure lipid system (data not shown); both diffusion coefficients were comparable to those determined for red blood cells (14). This showed that a fluid membrane bilayer can be formed by using this method, and that t-SNAREs reconstituted into target membranes do not affect phospholipid diffusion.

Pure Lipid Vesicles. Pure lipid vesicles containing 1.5 mol% each NBD-DPPE and Rh-DPPE in 82 mol% POPC/15 mol% 1,2-dioleoyl-*sn*-glycero-3-phosphatidylserine (DOPS) were prepared as described for POPC vesicles by bath sonication or by extrusion (LiposoFast, Avestin, Ottawa; 100-nm pore-size membrane, 31 passages). Both SUVs showed the same results independent of the preparation method.

Image Acquisition and Processing. TIR-FM was performed by using an inverted epifluorescence microscope (IX-70, Olympus, Melville, NY) equipped with a high-numerical-aperture (NA) objective (Apo \times 60 NA 1.45, Olympus) and a home-built temperature-controlling enclosure to maintain 37°C. The 514-nm laser line of an air-cooled tunable Argon laser (Omnichrome model 543-AP A01, Melles Griot) was reflected off a dichroic mirror (442/515dc, Chroma). Rh-DPPE was excited, and emission was collected through a 570 long-pass filter (Chroma). Because Rh is more photo-stable than NBD, only Rh-DPPE excitation and emission were used to monitor approach, docking, and fusion of v-liposomes to target membranes. Images were acquired with an ORCA-ER camera (Hamamatsu Photonics, Hamamatsu City, Japan) at exposure times of 100 ms (\pm 10% according to Universal Imaging). Elapsed rather than exposure time was used for data analysis. Camera, camera board (MV1500, Hamamatsu), and mechanical shutters (Uniblitz, Rochester, NY) were controlled by METAMORPH software. Images were streamed to memory. Image processing was done by using METAMORPH.

Dual-color imaging of Fluo-5N (10 μ M, K_d = 90 μ M, Molecular Probes) and Rh-DPPE was performed essentially as the single-color TIR experiments, except the 488-nm line of the tunable Argon laser and the laser light of a 543-nm HeNe laser (model 05-LGR-193, Melles Griot) were reflected by using a 488/543 dichroic mirror, and emission was collected by using a Dual-View splitter (Optical Insights, Santa Fe, NM) equipped with 515/30 band-pass filter to collect Fluo-5N emission, a 550

dichroic to split the emission, and a 580 long-pass filter to collect Rh-DPPE emission (all filters and dichroics are from Chroma).

Cleavage of VAMP-2 by Tetanus-Toxin (TeNT). Cleavage of VAMP-2 reconstituted in v-liposomes was performed with activated TeNT at 37°C for 30 min. The cleavage was verified by SDS/PAGE (data not shown). A control group of v-liposomes was kept at 37°C for 30 min, which did not influence the fusion probability when compared to another control not treated at a higher temperature (P = 0.48).

Results and Discussion

Approach, Docking, and Fusion of v-SNARE Proteoliposomes to Supported t-SNARE Bilayers. To study the role of neuronal SNAREs in membrane fusion, we used TIR-FM to monitor fusion of single vesicles containing v-SNARE proteins to a membrane containing t-SNARE proteins (for the schematic, see Fig. 6, which is published as supporting information on the PNAS web site). To mimic the target membrane, we prepared supported planar phospholipid bilayers on glass coverslips with the reconstituted t-SNARE proteins SNAP-25 and syntaxin 1A. To monitor fusion of v-liposomes (containing the v-SNARE VAMP-2) to the target membrane, Rh-DPPE incorporated into the v-liposome membrane was excited and its emission collected. This fluorophore was previously used together with NBD-DPPE in dequenching-based fusion assays (4).

TIR-FM ensured sufficient sensitivity to quantify the docking and fusion of individual v-liposomes (Fig. 1). The approach of v-liposomes to the supported target membrane was quantified by the increase in fluorescence intensity (the excitatory field in TIR-FM decays exponentially with a space constant of \approx 100 nm); fusion was quantified by delivery of Rh-DPPE fluorophores from the v-liposome membrane to, and the subsequent lateral diffusion in, the target membrane [Fig. 1 (6, 10)].

Upon addition, the v-liposomes rapidly entered the evanescent field and appeared at the target membrane (Fig. 1; Movie 1, which is published as supporting information on the PNAS web site). In the presence of divalent cations (here Ca^{2+}), these v-liposomes exhibited three distinct behaviors (Fig. 1A–C). For the largest population of v-liposomes, once they appeared in the evanescent field, their fluorescence remained unchanged (Fig. 1A and D), consistent with a v-liposome that is docked (criteria for docking: no movement) to the target membrane. Over the course of 800 ms, the v-liposome did not move or bleach significantly. For a second population of v-liposomes, the fluorescence transiently increased and then decreased (Fig. 1B and E), indicative of a v-liposome that approached the target membrane and then retreated (Fig. 2A). v-liposomes, when docked (Fig. 1D) or moving in and out of the evanescent field (Fig. 1E), do not show lateral spread of fluorescence.

A third population of v-liposomes showed a more complex fluorescence pattern (Fig. 1C, asterisk) characteristic of membrane fusion. The peak fluorescence transiently increased with no lateral spread (Fig. 1F, lines that represent each subsequent frame 100 ms apart, yellow, then orange, then red–orange), followed by a decrease of peak fluorescence, which is coincident with a lateral spread of fluorescence due to diffusion of fluorophores in the target membrane (Fig. 1F, red line, then brown line). As the peak fluorescence intensity decreased and the fluorescence spread, the total fluorescence intensity (integrated over the entire vesicle) continued to increase (Fig. 1C and F; Fig. 3A), which indicates that fluorophores were being delivered into the target membrane, where they were excited more effectively by the evanescent field. Over a longer period, the fluorophores diffused in the supported target bilayer, away from the site of fusion, thus the fluorescence returned to the background level (Fig. 1F, black line, t = 13.5 s). These fluorescence changes are consistent with v-liposomes fusing to the supported target mem-

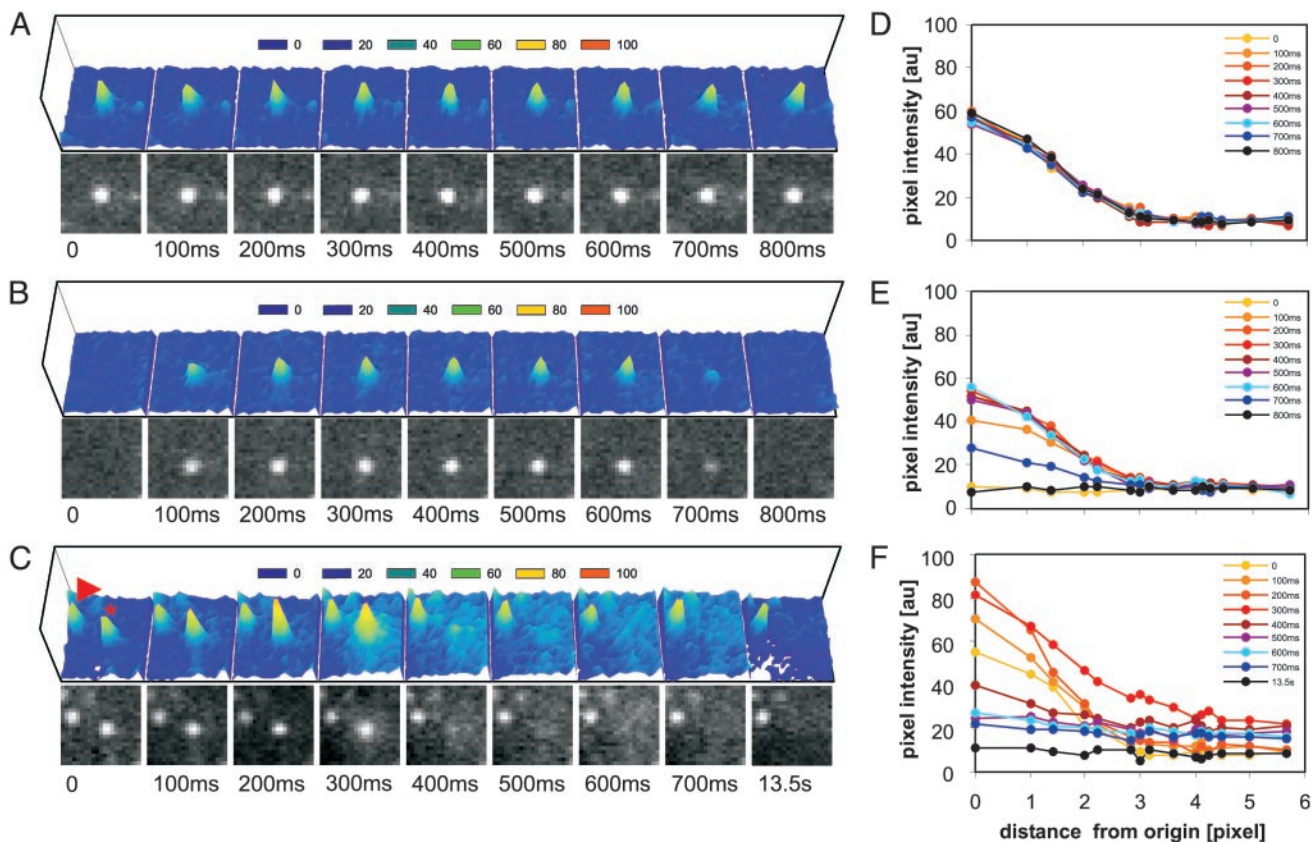


Fig. 1. Reconstituted membrane fusion by trans SNARE complexes revealed by single vesicle TIR-FM. (A) v-liposome is docked to a t-SNARE bilayer supported on glass. (B) v-liposome, which appears at the target membrane, stays, then disappears again, leaving no fluorescence at the target membrane. (C) Two v-liposomes are docked to the target membrane; one (marked by asterisk) fuses with the target membrane. The pseudocolored plots in A–C show in the z direction the fluorescence intensity [0–100 arbitrary units (au)] in 20-au steps from dark blue to orange of each pixel in the image field depicted below in gray scale (21×21 pixels, $21 \text{ pixels} = 2.3 \mu\text{m}$). The pixel intensity for the background was subtracted from raw data. (D–F) The lateral spread of fluorescence indicates fusion. The events in A–C are shown as average pixel intensity for pixels up to approximately six pixels in each direction from the origin (pixel with maximal intensity).

brane with kinetics < 1 s. Further, these observations exclude the following three alternative interpretations. (i) Photobleaching: The drop in peak intensity was not accompanied by a drop in total intensity. Also, there was no significant change in the peak and total fluorescence of an adjacent v-liposome of similar initial intensity that did not fuse (Fig. 1C, marked by an arrowhead). (ii) Lysis: The total fluorescence continued to increase even while the peak fluorescence decreased (Fig. 1C and F; Fig. 3A),

indicative of fluorophores being delivered into the target membrane where they are excited more effectively by the evanescent field. This rules out v-liposome lysis, because that would lead to diffusion of fluorophores away from the target membrane, hence a drop in total fluorescence intensity. Another possibility is lysis, then flattening, of the v-liposome membrane onto the target membrane. However, vesicle rupture produces a membrane lawn that is on top of, but not fused into, supported planar bilayers

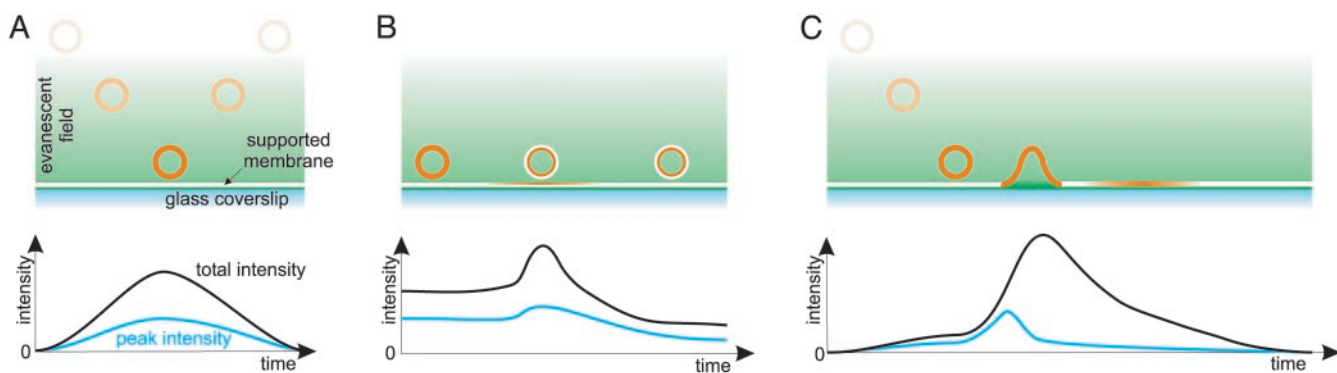


Fig. 2. Peak and total intensity courses (blue and black lines, respectively) over time for a fluorescently tagged liposome using TIR-FM that approaches the supported membrane bilayer, then docks and retreats (A); undergoes exchange of fluorophores from the outer leaflet to the upper leaflet of the supported membrane, which then diffuse away (B); and approaches the target membrane, docks, and then fuses (C). SNARE-mediated fusion of the two opposing membrane bilayers can be monitored by delivery and subsequent lateral spread of fluorescence in the supported target membrane (adapted from ref. 6).

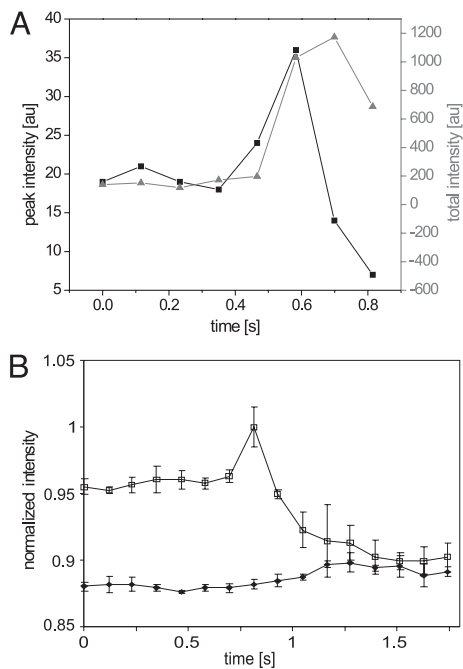


Fig. 3. (A) Quantified peak fluorescence (black) and total fluorescence intensity (gray) for a fusion event. (B) Normalized peak intensity for $n = 3$ fusing vesicles (open symbols) over time in comparison with background fluorescence (filled symbols). Means \pm SEM.

(15). (iii) Lipid exchange: The kinetics of inter- and intrabilayer transfer of fluorophore-tagged phosphatidylcholine show half-times of ≈ 350 s and ≈ 7.5 h, respectively (16). These rates are orders of magnitude slower than the rate of spread of fluorescence observed for this third population of v-liposomes. Because the v-liposome fluorophores (fluorescently tagged PE) are in both the inner and the outer leaflets, even if the interbilayer transfer of fluorophores occurs, the fluorescence would decrease to only approximately half its initial intensity, not to background levels as observed here (Figs. 1C, 2B, 3B, and 6).

SNARE Motifs Are Sufficient for Membrane Fusion in the Presence of Divalent Cations. Quantitative analysis of the parameters detailed in this assay allowed us to unambiguously identify fusion of proteoliposomes to target membranes. We thus used this assay to study the role of SNAREs and their domains on vesicle fusion (Fig. 4A).

In the absence of divalent cations, v-liposomes showed all of the above three behaviors exhibited by v-liposomes in the presence of Ca^{2+} (Fig. 1). However, in the absence of Ca^{2+} , fusion of v-liposomes containing VAMP-2 to a supported target membrane containing syntaxin and SNAP-25 was infrequent [Fig. 4A, $0.35 \pm 0.18\%$ of all docked v-liposomes fused to the target bilayer within a span of 50 s (% fusions/50 s)]. Increasing Ca^{2+} to $100 \mu\text{M}$ increased the fusion probability ≈ 40 -fold to $14.7 \pm 1.3\%$ fusions per 50 s ($P \approx 10^{-10}$). Increasing the concentration of another divalent cation, Mg^{2+} , instead of Ca^{2+} , to $100 \mu\text{M}$ increased the fusion probability ≈ 10 -fold to $3.6 \pm 1.7\%$ fusions per 50 s ($P < 0.01$), whereas 10 mM Mg^{2+} increased the fusion probability ≈ 20 -fold to $6.9 \pm 3.5\%$ fusions per 50 s ($P < 0.01$).

Divalent cations are known to bridge negatively charged phospholipid head groups such as phosphatidylserine as well as uncharged phosphatidylcholine head groups and have been reported to induce fusion between lipid vesicles (17–19). However, when the above experiments were repeated in the absence of SNARE proteins, no fusion events were observed in the

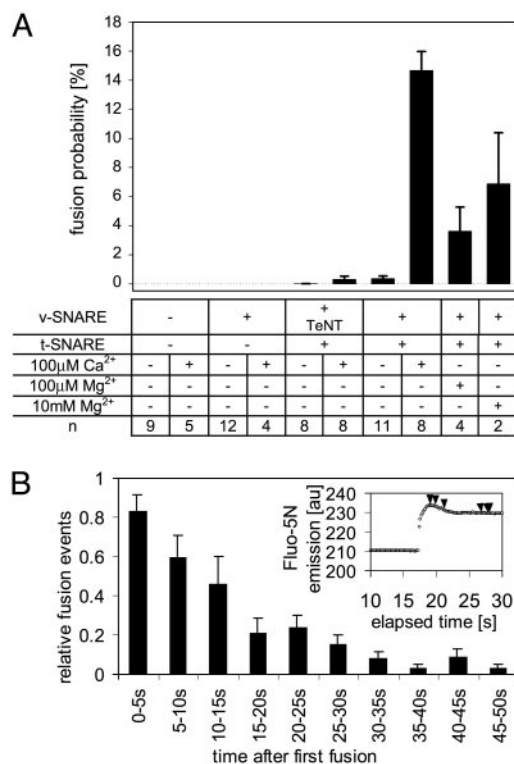


Fig. 4. (A) SNARE motifs in trans complexes are essential for membrane fusion. Shown is the number of fusing v-liposomes as percentage of all v-liposomes at the target membrane within the first 50 s of video streaming before addition of divalent cations or within 50 s after the addition of divalent cations. Error values represent SEM. (B) More than 50% of fusion-competent v-liposomes fuse within 10 s after Ca^{2+} addition. The bars represent means \pm SEM of normalized values for eight independent experiments (total of 696 fusion events); the final Ca^{2+} concentration was $100 \mu\text{M}$. (B Inset) The onset of Ca^{2+} -evoked fusion is fast. Using dual-color TIR-FM, the emission of Fluo-5N and Rh-DPPE-labeled v-liposomes was recorded simultaneously. Ca^{2+} was added after recording times > 10 s to establish baseline behavior. The plot shown is representative of four experiments. The final Ca^{2+} concentration used was $200 \mu\text{M}$.

absence of or after addition of Ca^{2+} to a final concentration of $100 \mu\text{M}$ (Fig. 4A). Further, no fusion events were observed even when VAMP-2 was reconstituted into proteoliposomes and tested with target membranes lacking t-SNAREs.

As a further test for the specific requirements for SNAREs in this fusion reaction, we used tetanus-toxin (TeNT), a Zn^{2+} -dependent protease known to cleave VAMP-2 at position 76 and release the N terminus containing the SNARE motif (20). A preparation of v-liposomes was divided in two halves, and one was treated with TeNT. In the absence of Ca^{2+} , the fusion probability was $0.007 \pm 0.007\%$ fusions per 50 s (Fig. 4A). Raising the Ca^{2+} level resulted in $0.32 \pm 0.21\%$ fusions per 50 s, but this change was not statistically significant ($P = 0.16$). In the presence of Ca^{2+} , VAMP-2 cleavage resulted in a ≈ 45 -fold reduction of fusion probability compared to uncleaved VAMP-2 ($14.7 \pm 1.3\%$ to $0.32 \pm 0.21\%$, $P \approx 10^{-8}$).

To characterize the temporal relationship between the increase of Ca^{2+} at the target membrane and the induction of fusion, fusions were monitored in the presence of the Ca^{2+} -sensitive dye Fluo-5N. Fusion always initiated as the emission of Fluo-5N fluorescence reached its maximum (Fig. 4B Inset). More than 50% of all Ca^{2+} -dependent fusions occurred within 10 s after the first fusion (Fig. 4B; 696 fusion events, eight independent experiments). Only $\approx 15\%$ of v-liposomes fused during the 50 s of recording (Fig. 4A; Movie 2, which is published

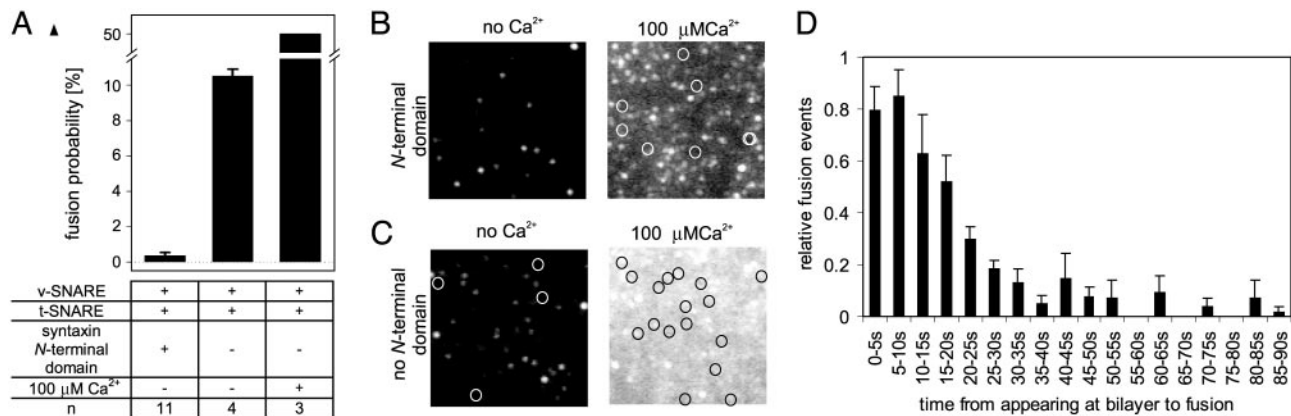


Fig. 5. The N-terminal H_{abc} domain of syntaxin acts as an inhibitor of fusion. (A) Fusion probability of v-liposomes to target membranes containing full-length syntaxin 1A and syntaxin without the N-terminal H_{abc} domain. Fusion probability represents the number of fusing v-liposomes as percentage of all docked v-liposomes within 50 s of video streaming or within 50 s after the addition of divalent cations. (B and C) Circles mark fusion events within 5 s before the frame shown, except (C Right) where fusions for the first 2 s of a 5-s span are circled. (D) Time spent by individual v-liposomes at the target membrane before Ca^{2+} -independent fusion is variable (total of 192 fusion events and four independent experiments).

as supporting information on the PNAS web site); longer recordings suggest that the remaining v-liposomes will not fuse even over tens of minutes (data not shown).

N-Terminal Domain of Syntaxin Has Inhibitory Effect on SNARE-Mediated Fusion. It has been demonstrated that the N terminus of syntaxin 1A regulates vesicle fusion kinetics (12, 21) and may play a direct regulatory role *in vivo* (22). To test this, v-liposomes were added to the target membrane containing syntaxin lacking the N-terminal H_{abc} domain. In the absence of added Ca^{2+} , the probability of spontaneous fusion in a span of 50 s ($10.5 \pm 0.4\%$) was ≈ 30 -fold higher with the truncated than with the full-length syntaxin ($0.35 \pm 0.18\%$, $P \approx 10^{-13}$) (Fig. 5A; Movie 3, which is published as supporting information on the PNAS web site). Raising Ca^{2+} to $100 \mu M$ further increased the fusion probability. Due to the fusion of excessive numbers of v-liposomes, the increase in fluorescence of the target membrane precluded visualization of individual v-liposomes and hence quantification (Movie 4, which is published as supporting information on the PNAS web site). However, based on the docked v-liposomes remaining after Ca^{2+} addition, we estimated that removal of the syntaxin H_{abc} domain caused $>50\%$ of docked v-liposomes to fuse during the first 50 s (Fig. 5A). Examples of such experiments are shown in Fig. 5B and C. Fusion events are circled. In one representative case, in the absence of added Ca^{2+} , four v-liposomes fused to target membrane containing the truncated syntaxin within 5 s (Fig. 5C Left), whereas no fusion was detectable with full-length syntaxin within this time frame (Fig. 5B Left). Increase of Ca^{2+} to $100 \mu M$ caused eight fusions in 5 s (Fig. 5B Right). Twice as many v-liposomes fused in only 2 s to target membrane containing truncated syntaxin (Fig. 5C Right). The massive increase in fluorescence intensity of the target membrane containing truncated syntaxin due to Ca^{2+} -dependent fusion of excessive numbers of v-liposomes is evident (Fig. 5C Right).

The docking time for each v-liposome at the target membrane containing truncated syntaxin was analyzed by quantifying the rate of spontaneous (Ca^{2+} -independent) fusion of v-liposomes to these target membranes (Fig. 5D). More than 70% of all fusing v-liposomes (192 fusion events, four independent experiments) were docked for <20 s; some v-liposomes were docked for <1 s before fusing to the target membrane. Docking times >35 s occurred for $<15\%$ of fusing v-liposomes. This distribution of docking times is similar to the distribution of latencies to fusion quantified for full-length syntaxin after addition of Ca^{2+} (Fig.

4A). This suggests there may be a similar rate-limiting step for both, Ca^{2+} -evoked fusion mediated by full-length syntaxin and Ca^{2+} -independent fusion after removal of the H_{abc} domain of syntaxin.

During a 50-s period, $<20\%$ of the v-liposomes fused in the presence of full-length syntaxin and Ca^{2+} . This limited fusion competency could be due to variations in VAMP-2 concentration or proteoliposome size, thus curvature, across the proteoliposome population. Alternatively, t-SNARE concentration in the target bilayer may be limiting at fusion sites with sufficient t-SNAREs for docking but not for fusion. A third possibility is that the H_{abc} domain of syntaxin may leave many of the molecules in a refractory state for fusion. When this domain was cleaved, the fusion efficiency increased significantly. A regulatory role of the H_{abc} domain of syntaxin on membrane fusion has been suggested (12, 21, 22). Our results provide further evidence toward an inhibitory effect of the H_{abc} domain on membrane fusion even without further regulatory proteins such as Munc13 and Munc18, which are believed to interact with the H_{abc} domain of syntaxin and regulate SNARE complex assembly, thus membrane fusion (1, 23–25).

Kinetics of Membrane Fusion. The SNARE-mediated fusion reaction that we report here is unexpectedly much faster than previously observed (4). The protein and phospholipid compositions are virtually identical in the two assays, but the geometry is radically different. Solution phase fusion involves ≈ 50 -nm diameter proteoliposomes containing reconstituted SNAREs, whereas in the present study, one of the partners is large and flat (as is typically the case in a cell).

A critical issue is whether the reconstituted system can recapitulate the kinetics of fusion observed *in vivo*. The very first release of neurotransmitter can be detected $200 \mu s$ after the rise of Ca^{2+} in the presynaptic terminal (26). However, release continues afterward for many tens to hundreds of milliseconds. The initial opening of the fusion pore has been monitored by capacitance; the pore flickers open and closed for 10–15,000 ms before it starts to expand (27–30). The pore may continue to widen for hundreds of milliseconds before the vesicle is flattened into the plasma membrane. Our observation that individual fusion events between v-SNARE vesicles and the t-SNARE target membrane initiate <100 ms after the rise of Ca^{2+} (Fig. 4B Inset), and that the vesicular membrane has intermixed with the target membrane in 300 ms (Fig. 1F), establishes that the

SNARE machinery is kinetically competent to mediate fast fusion processes in cells.

This assay allows us to quantify the steps and kinetics of SNARE-mediated fusion, including rates and duration of docking, rates of liposome flattening, and lipid mixing during fusion. Thus, we can test the quantitative effects of divalent cations, variations in lipid (e.g., varying the amount of negatively charged phospholipids such as phosphatidylserine), and variations of protein (e.g., replacing SNAP-25 with SNAP-23) on this process. Further, we can test the roles of accessory proteins on the inhibitory effects of the N terminus of syntaxin as well as assess even subtle contributions of each of the SNARE proteins.

By imaging individual fusion events, we have demonstrated the occurrence of SNARE-mediated fusion and membrane mixing. This approach also allowed us to unambiguously rule out the formal possibility of interbilayer lipid transfer. We demonstrate that the presence of divalent cations is insufficient to allow detectable membrane fusion in the absence of both v- and t-SNAREs. Although our results do not distinguish whether the divalent cations directly function at the level of phospholipids, on

one of the SNAREs, or a combination thereof (31, 32), we detected that even the minimal fusion machinery is sensitive to the presence of divalent cations. The concentrations of Ca^{2+} used are similar to the values calculated to occur just under the plasma membrane of the presynaptic terminal (33) and are consistent with the measurement of $194 \mu\text{M}$ as the concentration of Ca^{2+} to give half-maximal exocytosis (34). This suggests that SNAREs together with Ca^{2+} and lipids might be the minimal Ca^{2+} -dependent fusion machinery. Other regulatory factors may function to activate or inhibit this machinery.

The ability to examine single fusion events in real-time with complete control over lipid and protein composition promises to reveal new insights into the mechanisms that can accomplish this remarkable degree of regulation.

We thank Joshua Zimmerberg for helpful comments on the manuscript and Michael Wollenberg for technical assistance. This work was supported by National Institutes of Health Grants R01 DK27044 (to J.E.R.), R01 NS043391 (to T.H.S.), and 1F32GM069200 (to J.Z.R.), and National Science Foundation Grants BES 0110070 and BES 0119468 (to S.M.S.).

1. Söllner, T. H. (2003) *Mol. Membr. Biol.* **20**, 209–220.
2. Ungar, D. & Hughson, F. M. (2003) *Annu. Rev. Cell Dev. Biol.* **19**, 493–517.
3. Hu, C., Ahmed, M., Melia, T. J., Söllner, T. H., Mayer, T. & Rothman, J. E. (2003) *Science* **300**, 1745–1749.
4. Weber, T., Zemelman, B. V., McNew, J. A., Westermann, B., Gmachl, M., Parlati, F., Söllner, T. H. & Rothman, J. E. (1998) *Cell* **92**, 759–772.
5. Oheim, M., Loerke, D., Stühmer, W. & Chow, R. H. (1998) *Eur. Biophys. J.* **27**, 83–98.
6. Schmoranzler, J., Goulian, M., Axelrod, D. & Simon, S. M. (2000) *J. Cell Biol.* **149**, 23–31.
7. Johns, L. M., Levitan, E. S., Shelden, E. A., Holz, R. W. & Axelrod, D. (2001) *J. Cell Biol.* **153**, 177–190.
8. Yang, D. M., Huang, C. C., Lin, H. Y., Tsai, D. P., Kao, L. S., Chi, C. W. & Lin, C. C. (2003) *J. Microsc.* **209**, 223–227.
9. Kreitzer, G., Schmoranzler, J., Low, S. H., Li, X., Gan, Y. B., Weimbs, T., Simon, S. M. & Rodriguez-Boulan, E. (2003) *Nat. Cell Biol.* **5**, 126–136.
10. Jaiswal, J. K., Andrews, N. W. & Simon, S. M. (2002) *J. Cell Biol.* **159**, 625–635.
11. Hinterdorfer, P., Baber, G. & Tamm, L. K. (1994) *J. Biol. Chem.* **269**, 20360–20368.
12. Parlati, F., Weber, T., McNew, J. A., Westermann, B., Söllner, T. H. & Rothman, J. E. (1999) *Proc. Natl. Acad. Sci. USA* **96**, 12565–12570.
13. Wagner, M. L. & Tamm, L. K. (2001) *Biophys. J.* **81**, 266–275.
14. Koppel, D. E., Sheetz, M. P. & Schindler, M. (1981) *Proc. Natl. Acad. Sci. USA* **78**, 3576–3580.
15. Wong, A. P. & Groves, J. T. (2002) *Proc. Natl. Acad. Sci. USA* **99**, 14147–14152.
16. Bai, J. N. & Pagano, R. E. (1997) *Biochemistry* **36**, 8840–8848.
17. Feigenson, G. W. (1989) *Biochemistry* **28**, 1270–1278.
18. Altenbach, C. & Seelig, J. (1984) *Biochemistry* **23**, 3913–3920.
19. Düzgünes, N., Nir, S., Wilschut, J., Bentz, J., Newton, C., Portis, A. & Papahadjopoulos, D. (1981) *J. Membr. Biol.* **59**, 115–125.
20. Schiavo, G., Benfenati, F., Poulain, B., Rossetto, O., Delauroto, P. P., Das-Gupta, B. R. & Montecucco, C. (1992) *Nature* **359**, 832–835.
21. Dulubova, I., Sugita, S., Hill, S., Hosaka, M., Fernandez, I., Südhof, T. C. & Rizo, J. (1999) *EMBO J.* **18**, 4372–4382.
22. Dietrich, L. E. P., Boeddinghaus, C., LaGrassa, T. J. & Ungermann, C. (2003) *Biochim. Biophys. Acta* **1641**, 111–119.
23. Rizo, J. & Südhof, T. C. (2002) *Nat. Rev. Neurosci.* **3**, 641–653.
24. Li, L. & Chin, L. S. (2003) *Cell. Mol. Life Sci.* **60**, 942–960.
25. Gerst, J. E. (2003) *Biochim. Biophys. Acta* **1641**, 99–110.
26. Llinás, R., Steinberg, I. Z. & Walton, K. (1981) *Biophys. J.* **33**, 323–351.
27. Neher, E. & Marty, A. (1982) *Proc. Natl. Acad. Sci. USA* **79**, 6712–6716.
28. Curran, M. J., Cohen, F. S., Chandler, D. E., Munson, P. J. & Zimmerberg, J. (1993) *J. Membr. Biol.* **133**, 61–75.
29. Spruce, A. E., Breckenridge, L. J., Lee, A. K. & Almers, W. (1990) *Neuron* **4**, 643–654.
30. Dernick, G., Alvarez de Toledo, G. & Lindau, M. (2003) *Nat. Cell Biol.* **5**, 358–362.
31. Sørensen, J. B., Matti, U., Wei, S. H., Nehring, R. B., Voets, T., Ashery, U., Binz, T., Neher, E. & Rettig, J. (2002) *Proc. Natl. Acad. Sci. USA* **99**, 1627–1632.
32. Kweon, D. H., Kim, C. S. & Shin, Y. K. (2003) *Nat. Struct. Biol.* **10**, 440–447.
33. Simon, S. M. & Llinás, R. R. (1985) *Biophys. J.* **48**, 485–498.
34. Heidelberger, R., Heinemann, C., Neher, E. & Matthews, G. (1994) *Nature* **371**, 513–515.